OXFORD

SOT | Society of Toxicology
www.toxsci.oxfordjournals.org

TOXICOLOGICAL SCIENCES, 2017, 1–12

doi: 10.1093/toxsci/kfw259
Advance Access Publication Date: December 20, 2016
Research Article

BDE-47 and BDE-49 Inhibit Axonal Growth in Primary Rat Hippocampal Neuron-Glia Co-Cultures via Ryanodine Receptor-Dependent Mechanisms

Hao Chen,* Karin M. Streifel,* Vikrant Singh,† Dongren Yang,* Linley Mangini,* Heike Wulff,† and Pamela J. Lein*,[1]

*Department of Molecular Biosciences, School of Veterinary Medicine; and †Department of Pharmacology, School of Medicine, University of California-Davis, Davis, California 95616

[1]To whom correspondence should be addressed at Department of Molecular Biosciences, School of Veterinary Medicine, University of California, Davis, 1089 Veterinary Medicine Drive, Davis, CA 95616. Fax: (530) 752-7690. E-mail: pjlein@ucdavis.edu.

ABSTRACT

Polybrominated diphenyl ethers (PBDEs) are widespread environmental contaminants associated with adverse neurodevelopmental outcomes in children and preclinical models; however, the mechanisms by which PBDEs cause developmental neurotoxicity remain speculative. The structural similarity between PBDEs and nondioxin-like (NDL) polychlorinated biphenyls (PCBs) suggests shared toxicological properties. Consistent with this, both NDL PCBs and PBDEs have been shown to stabilize ryanodine receptors (RyRs) in the open configuration. NDL PCB effects on RyR activity are causally linked to increased dendritic arborization, but whether PBDEs similarly enhance dendritic growth is not known. In this study, we quantified the effects of individual PBDE congeners on not only dendritic but also axonal growth since both are regulated by RyR-dependent mechanisms, and both are critical determinants of neuronal connectivity. Neuronal-glial co-cultures dissociated from the neonatal rat hippocampus were exposed to BDE-47 or BDE-49 in the culture medium. At concentrations ranging from 20 pM to 2 μM, neither PBDE congener altered dendritic arborization. In contrast, at concentrations $\geq$ 200 pM, both congeners delayed neuronal polarization resulting in significant inhibition of axonal outgrowth during the first few days *in vitro*. The axon inhibitory effects of these PBDE congeners occurred independent of cytotoxicity, and were blocked by pharmacological antagonism of RyR or siRNA knockdown of RyR2. These results demonstrate that the molecular and cellular mechanisms by which PBDEs interfere with neurodevelopment overlap with but are distinct from those of NDL PCBs, and suggest that altered patterns of neuronal connectivity may contribute to the developmental neurotoxicity of PBDEs.

Key words: axon; calcium signaling; developmental neurotoxicity; neuronal morphogenesis; PBDE; ryanodine receptor.

Polybrominated diphenyl ethers (PBDEs), synthetic brominated compounds that were used extensively as flame retardants in consumer products, have become persistent and ubiquitous environmental contaminants. PBDE levels in human tissues have increased significantly over the past 3 decades, and body burdens are significantly higher in infants and toddlers relative to adults (EFSA, 2011; USEPA, 2010). Epidemiological studies report an association between early-life PBDE exposure and neurobehavioral deficits, including decreased attention, poorer performance on intelligence indices, psychomotor deficits, and increased activity/impulsivity (Berghuis *et al.*, 2015). Preclinical studies confirm that developmental PBDE exposures can cause persistent neurobehavioral deficits (Costa *et al.*, 2014; Hendriks and Westerink, 2015).

PBDEs have been reported to interfere with thyroid hormone function, alter Ca^{2+} homeostasis, cause oxidative stress and modulate cholinergic, glutamatergic, and GABAergic neurotransmission (Costa *et al.*, 2014; Dingemans *et al.*, 2011; Hendriks

and Westerink, 2015). However, it is not clear whether or how these molecular effects relate to PBDE-induced neurobehavioral deficits. One hypothesis is that PBDEs cause developmental neurotoxicity by interfering with normal patterns of neuronal connectivity (Kodavanti and Curras-Collazo, 2010; Stamou *et al.*, 2013). This hypothesis is derived from the following observations: (1) thyroid hormone, Ca^{2+}, reactive oxygen species (ROS) and neurotransmitter-dependent signaling mechanisms are well known to influence the development of neuronal connectivity via dynamic control of axonal and dendritic morphogenesis (Chandrasekaran *et al.*, 2015; Goldberg, 2003; Kapfhammer, 2004; Lohmann and Wong, 2005; Valnegri *et al.*, 2015); and (2) dysregulated axonal or dendritic growth is linked to impaired behavior in preclinical models (Berger-Sweeney and Hohmann, 1997), and to multiple neurodevelopmental disorders in humans, including autism spectrum disorders, attention deficit hyperactivity disorder and schizophrenia (Copf, 2016; Robichaux and Cowan, 2014).

In further support of this hypothesis, we previously demonstrated that PBDE congeners with more than one *ortho* bromine substitution interact with the ryanodine receptor (RyR) to promote Ca^{2+} release from intracellular stores (Kim *et al.*, 2011). RyRs are Ca^{2+} channels that regulate Ca^{2+} release from the endoplasmic reticulum (Pessah *et al.*, 2010), and RyR function is required for activity-dependent dendritic growth (Adasme *et al.*, 2011; Ohashi *et al.*, 2014; Wayman *et al.*, 2012b) and for axonal growth and guidance (Wilson *et al.*, 2016). Nanomolar concentrations of nondioxin-like (NDL) polychlorinated biphenyls (PCBs), which are structurally similar to PBDEs and proposed to share toxicological modes of action (Kodavanti and Curras-Collazo, 2010), also interact with RyR1 and RyR2 to sensitize their activation by submicromolar levels of Ca^{2+} and attenuate their inhibition by micromolar levels of Ca^{2+} and Mg^{2+} (Wong *et al.*, 1997a; Wong and Pessah, 1996). NDL PCB interactions with RyR stabilize the receptor in its open configuration (Samso *et al.*, 2009), which increases intracellular levels of Ca^{2+} (Wayman *et al.*, 2012a). NDL PCB sensitization of RyRs is causally linked to enhanced dendritic arborization in hippocampal and cortical neurons (Wayman *et al.*, 2012b; Yang *et al.*, 2009, 2014) via activation of Ca^{2+}-dependent signaling pathways (Wayman *et al.*, 2012a). Although PBDEs were recently reported to alter axonal growth in larval zebrafish (Chen *et al.*, 2012), whether PBDEs influence axonal or dendritic morphogenesis in mammalian central neurons via RyR-dependent mechanisms has not been previously evaluated.

Here, we address this question by exposing primary cultures of rat hippocampal neurons to either BDE-47, a PBDE congener with relatively weak RyR activity (Kim *et al.*, 2011) that is highly abundant in human tissues (USEPA, 2010), or BDE-49, a PBDE congener with relatively potent RyR activity (Kim *et al.*, 2011) that has been detected in gestational tissues from women in southeast Michigan at levels comparable to BDE-47 (Miller *et al.*, 2009). Our findings indicate that while neither congener alters dendritic arborization, both decrease axonal growth with comparable potency via RyR-dependent mechanisms.

MATERIALS AND METHODS

Materials

Neat certified BDE-47 (2,2′,4,4′-tetrabromodiphenyl ether, >99% pure), BDE-49 (2,2′,4,5′-tetrabromodiphenyl ether, > 99% pure), and 4′-OH-BDE-49 (97.8% pure) were purchased from AccuStandard Inc. (New Haven, Connecticut), and verified for purity and composition by GC/MS by the UC Davis Superfund Research Program Analytical Core. 6-OH-BDE-47 was a gift from Dr Ellen Fritsche (IUF—Leibinz Research Institute for Environmental Medicine, Düsseldorf, Germany). Stock solutions of each BDE were made in dry dimethyl sulfoxide (DMSO, Sigma-Aldrich, St Louis, Missouri). Paraformaldehyde was purchased from Sigma-Aldrich. FLA365 (4-(2-aminopropyl)-3,5-dichloro-*N*,*N*-dimethylaniline) was synthesized as previously described in Florvall *et al.* (1977) and confirmed to be >99% pure by NMR (see Supplementary Materials). Xestospongin C was purchased from Cayman Chemical (Ann Arbor, Michigan); verapamil hydrochloride, from Sigma-Aldrich. Microtubule-associated protein-2B-enhanced green fluorescent protein (MAP2B-eGFP) and pCAG-tomato fluorescent protein constructs were generous gifts from Dr Gary Wayman (Washington State University, Pullman, Waltham) and their synthesis and characterization have been previously published (Wayman *et al.*, 2006).

Animals

All procedures involving animals were conducted according to protocols approved by the Institutional Animal Care and Use Committee of the University of California, Davis. Timed-pregnant Sprague Dawley rats were purchased from Charles River Laboratory (Hollister, California) and individually housed in clear plastic cages with corn cob bedding. Food and water were provided *ad libitum*. Temperatures were maintained at 22 ± 2°C throughout a 12-h light–dark cycle.

Cell Culture

Primary hippocampal cell cultures were prepared from postnatal day (P) 0 or P1 male and female rat pups (hippocampi from male and female pups were pooled) as previously described in Wayman *et al.* (2006). Briefly, dissociated hippocampal cells were plated on glass coverslips (Bellco Glass, Vineland, New Jersey) precoated with poly-L-lysine (0.5 mg/ml, Sigma-Aldrich) and maintained at 37°C in NeuralQ Basal Medium supplemented with 2% GS21 (MTI-GlobalStem, Gaithersburg, Maryland) and GlutaMAX (ThermoScientific, Waltham, Massachusetts). For studies of neuronal cell polarization, axonal morphogenesis and intracellular Ca^{2+} levels, cells were plated at 33 000 cells/cm^2; for studies of dendritic growth, at 83 000 cells/cm^2. Phase contrast images of cultures grown at either cell density are provided in Supplementary Figure S2. For all PBDE exposure experiments, cultures were exposed to BDE-47 or BDE-49 diluted in culture medium from 1000× stocks; control cultures were exposed to vehicle (DMSO; 1:1000 dilution). A broad concentration range of BDE-47 and BDE-49 (20 pM–2 μM) was tested in initial experiments to evaluate the effects of individual PBDE congeners on dendritic arborization, axonal morphogenesis and cell viability to determine concentration-response relationships. In subsequent experiments designed to investigate the role of specific signaling molecules in mediating the effects of PBDEs on axonal growth, BDE-47 and BDE-49 were used at 200 nM because, across all dissections, this was the highest concentration that consistently inhibited axonal growth in the absence of any evidence of cytotoxicity. For studies of neuronal cell polarization and early stages of axonal growth, cultures were exposed for 48 h beginning 3 h after plating; for studies of intracellular Ca^{2+} levels, cultures were acutely exposed on day *in vitro* (DIV) 2; for studies of dendritic growth and late stages of axonal growth, cultures were exposed for 48 h beginning on DIV 7.

siRNA Knockdown

Construct sequences and specificity of RyR1 siRNA, RyR2 siRNA and control (scrambled) siRNA were previously published (Wayman *et al.*, 2012b). In this study, siRNA were fluorescently labeled using LabelIT (Mirus, Madison Wisconsin) per the manufacturer's instructions in order to identify transfected cells. To transfect hippocampal neurons, freshly dissociated hippocampal cells were electroporated with siRNA prior to plating using the Amaxa Nucleofector (Amaxa Biosystems, Lonza) according to the manufacturer's protocol. Transfection efficiency was approximately 40%.

Morphometric Analyses

To visualize the dendritic arbor, hippocampal cultures were transfected on DIV 6 with a pCAGGS expression vector encoding a MAP2B-eGFP fusion construct (Wayman *et al.*, 2006), using Lipofectamine-2000 (Invitrogen, Carlsbad, California) according to the manufacturer's protocol. Transfection efficiency ranged between 0.1 and 0.2%, which is desirable for morphometric analyses. Dendritic lengths were quantified from digital images of GFP+ neurons using ImageJ software with the NeuronJ plugin (Meijering *et al.*, 2004) by an individual blinded to experimental condition. Total dendritic length was measured in at least 30 neurons from 3 coverslips per treatment group, and the experiment was repeated at least 3 times with cultures prepared from independent dissections.

To quantify axonal morphology, cultures were fixed with 4% paraformaldehyde then reacted with antibody specific for tau-1 (1:1000, Millipore, Billerica, Massachusetts) to visualize axons. Axonal lengths were quantified in tau-1 immunopositive neurons by an individual blinded to experimental condition using ImageJ software with the NeuronJ plugin. As previously defined (Dotti *et al.*, 1988; Lein *et al.*, 1992), a neurite was considered an axon if its length was at least 2.5 times the diameter of the cell body, and it exceeded in length all other neurites extended by the same neuron. Total axonal length was measured in at least 30 neurons from 3 coverslips per treatment group, and the experiment was repeated in cultures prepared from 3 independent dissections.

To assess neuronal cell polarity, cultures were reacted with GAP-43 antibody (1:1000, Millipore, Billerica, Massachusetts). Polarity was scored in GAP-43 immunopositive neurons by an individual blinded to treatment using previously described stages (Goslin *et al.*, 1990). The experiment was repeated in cultures prepared from 3 independent dissections.

Cytotoxicity Analyses

Cytotoxicity was assessed by quantifying lactate dehydrogenase (LDH) released into the culture medium (Mosmann, 1983) using the CytoTox-ONE Homogenous Membrane Integrity Assay (Promega, Madison, Wisconsin, USA) per the manufacturer's directions. Cell viability was also assessed in independent cultures by reacting cultures with calcein-AM (0.25 μM; Invitrogen) and propidium iodide (1.25 μM; Sigma-Aldrich) to identify live and dead cells, respectively. The number of live (calcein-AM-labeled) and dead (propidium iodide-labeled) cells was determined using an automated high content imaging system (ImageExpress, Molecular Devices, Sunnyvale, California). Data are expressed as a % of viable cells as determined by the following formula: 100 X [(no. calcein-AM-labeled cells)/(no. calcein-AM-labeled + no. propidium iodide-labeled cells)]. Cytotoxicity was assayed in 12 wells per treatment and experiments were repeated using cultures obtained from 3 independent dissections. Data are expressed as a % of vehicle control values from the same dissection.

Western Blot Analysis of Tau-1

At DIV 7, low-density cultures were treated with BDE-47 or BDE-49 for 48 h, then lysed with ice-cold RIPA buffer (150 mM NaCl, 1.0% NP-40, 0.5% sodium deoxycholate, 0.1% SDS in 50 mM Tris, pH 8.0 with Halt protease inhibitor) at DIV 9. Protein concentrations of the lysates were determined using the bicinchoninic acid (BCA) Protein Assay (Pierce, Rockford Illinois). An equal amount of protein (10 μg) of each sample was separated by 12% SDS-PAGE, and transferred to PDVF membrane. Membranes were blocked for 1 h in Odyssey Blocking Buffer (LI-COR, Lincoln NE) then incubated overnight at 4°C with antibodies specific for tau-1 (1:1000, Millipore, Billerica, Massachusetts) and GAPDH (1:1000, Cell Signaling Technology Danvers, Massachusetts) prepared in blocking buffer. After PBS wash, membranes were incubated with secondary antibodies conjugated to infrared dye IR700 or IR800 for 1 h at room temperature and then washed with PBS. Membranes were scanned and densitometric values obtained using the Odyssey Infrared Imaging System (LI-COR, Lincoln NE). The densitometric value for each tau-1 immunopositive band was normalized to the densitometric value for the GAPDH immunopositive band within the same sample.

Immunocytochemical Localization of RyR

To confirm RyR expression in the axonal growth cone, cultures were fixed with 4% paraformaldehyde on DIV 2, permeabilized with 0.1% Triton X-100 for 5 min, incubated in blocking buffer containing 5% fetal bovine serum, 0.05 M NH_4Cl, 2% glycerol, and 2% goat serum for 1 h and then reacted overnight with RyR1-selective antibody 34C (1:100, Developmental Studies Hybridoma Bank, Iowa City, Iowa) or RyR2-selective antibody C3-33 (1:100, Abcam, Cambridge, Massachusetts). After PBS wash, Alexa Fluor dyes (1:1000, Molecular Probes, Invitrogen) and Oregon-Green phalloidin (1:1000, ThermoScientific) were applied for 1 h.

Statistical Analysis

All data are presented as mean ± SE. Graphs and statistical analyses were performed with GraphPad Prism 4.0. Data were analyzed using 1-way *ANOVA* with Tukey's or Dunnett's *post hoc* or with Kruskal-Wallis with Dunn's *post hoc* as appropriate. Datasets were log transformed for statistical analysis if they did not pass the Shapiro-Wilk test of normality.

RESULTS

BDE-47 and BDE-49 Selectively Interfere with Axonal Growth in Primary Hippocampal Neurons

We have previously shown that NDL-PCBs enhance dendritic arborization in cultured hippocampal neurons via RyR-dependent mechanisms (Wayman *et al.*, 2012b; Yang *et al.*, 2014). Therefore, we predicted that BDE-47 and BDE-49, which exhibit relatively low versus relatively high RyR activity, respectively (Kim *et al.*, 2011), would exhibit weak versus robust dendrite promoting activity. To visualize dendritic arbors of individual neurons in high-density neuron-glia co-cultures dissociated from P0 to P1 rat hippocampi, cultures were transfected with a MAP2B-eGFP construct under the control of the

neuron-specific CAG promoter (Wayman *et al.*, 2006). Expression of MAP2B-eGFP is restricted to the somatodendritic compartment in cultured hippocampal neurons and does not alter their intrinsic dendritic growth patterns (Wayman *et al.*, 2006). Under the culture conditions used for these experiments, the dendritic arbor expands most rapidly between DIV 5 and 10 (Wayman *et al.*, 2006); therefore, cultures were transfected with MAP2B-eGFP on DIV 6, then exposed from DIV 7 to 9 to varying concentrations of BDE-47 or BDE-49. Control cultures were exposed to vehicle (DMSO at 1:1000 dilution) or, as a positive control, to PCB 95 (200 nM). We previously demonstrated that PCB 95, a NDL-PCB with potent activity at the RyR, significantly enhances dendritic arborization in cultured hippocampal neurons (Wayman *et al.*, 2012b). Consistent with previous studies (Wayman *et al.*, 2012b), neurons exposed to PCB 95 had a more complex dendritic arbor (Figure 1A), evidenced as a significant increase in total dendritic length per neuron relative to vehicle control neurons (Figure 1B). In contrast, the dendritic arborization of neurons exposed to either BDE-47 or BDE-49 at concentrations ranging from 200 pM to 2 μM was not significantly different from that of neurons exposed to vehicle (Figs. 1A and B).

RyRs are expressed not only in dendrites (Seymour-Laurent and Barish, 1995; Wayman *et al.*, 2012b), but also in axons (Hertle and Yeckel, 2007), and RyR activity has been implicated in the regulation of axonal growth and guidance (Wilson *et al.*, 2016). Therefore, we examined whether PBDEs alter axonal growth in primary hippocampal neurons. For studies of axonal growth, primary hippocampal cell cultures were plated at a lower cell density and exposed to BDE-47 or BDE-49 for 48 h beginning 3 h after plating in order to visualize the complete axonal plexus of individual neurons (Yang *et al.*, 2014). At the end of the exposure period, cultures were fixed and immunostained for tau-1, which is an axon-selective cytoskeleton-associated protein (Hayashi *et al.*, 2002). Exposure to either BDE-47 or BDE-49 did not change the number of axons extended by cultured hippocampal neurons but did significantly decrease the length of axons (Figure 2A). Morphometric analyses indicated that at concentrations ranging from 200 pM to 2 μM, both PBDE congeners significantly decreased axonal length by 15–25% relative to vehicle control values while neither PBDE congener altered axonal growth at 20 pM (Figure 2B). Since a classic sigmoidal shaped concentration-effects was not observed in these experiments, we next exposed cultures to BDE-47 or BDE-49 at concentrations ranging from 25 to 100 pM to determine whether our initial experiments missed a steep concentration-effect curve. However axonal lengths were not significantly different from vehicle controls in cultures exposed to PBDE concentrations ranging from 25 to 100 pM (Supplementary Figure S3). Hydroxylated metabolites of BDE-47 and BDE-49 have also been shown to sensitize RyRs (Kim *et al.*, 2011), and to be more potent than the parent compounds in increasing $[Ca_i^{2+}]$ in PC12 cells (Dingemans *et al.*, 2008). Exposure to 6-OH-BDE-47 and 4′-OH-BDE-49 at concentrations ranging from 0.1 to 100 nM caused a significant decrease in axonal length only in cultures exposed to the highest concentration (100 nM) of either PBDE congener (Figure 2C).

To determine whether PBDE effects on axonal growth are a secondary effect of cytotoxicity, cell viability was assessed in PBDE-exposed cultures using 2 assays that measure different

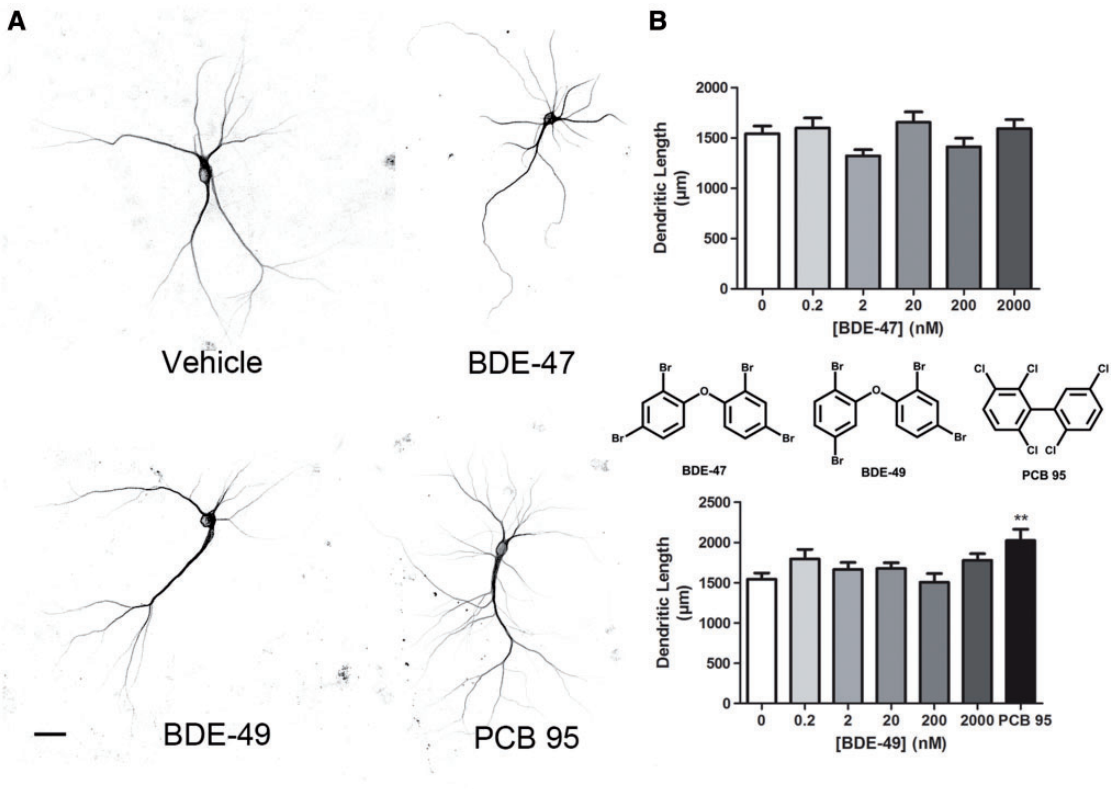

FIG. 1. BDE-47 and BDE-49 do not alter dendritic growth in cultured hippocampal neurons. Cells dissociated from P1 rat hippocampi were transfected with MAP2B-eGFP at DIV 6. On DIV 7, cultures were exposed to vehicle (DMSO diluted 1:1000) or varying concentrations of BDE-47 or BDE-49 for 48 h. **A,** Representative photomicrographs of DIV 9 neurons expressing MAP2B-eGFP following exposure to vehicle, BDE-47 (200 nM) or BDE-49 (200 nM). PCB 95 (200 nM) was added to a subset of cultures as a positive control. **B,** Quantification of dendritic length in GFP+ neurons. Data from one experiment presented as the mean ± SE (n = 30–40 neurons per condition). Experiments were repeated in 3 independent dissections with comparable results from each experiment. *$P < .05$ relative to vehicle control. Scale bar = 25 μm.

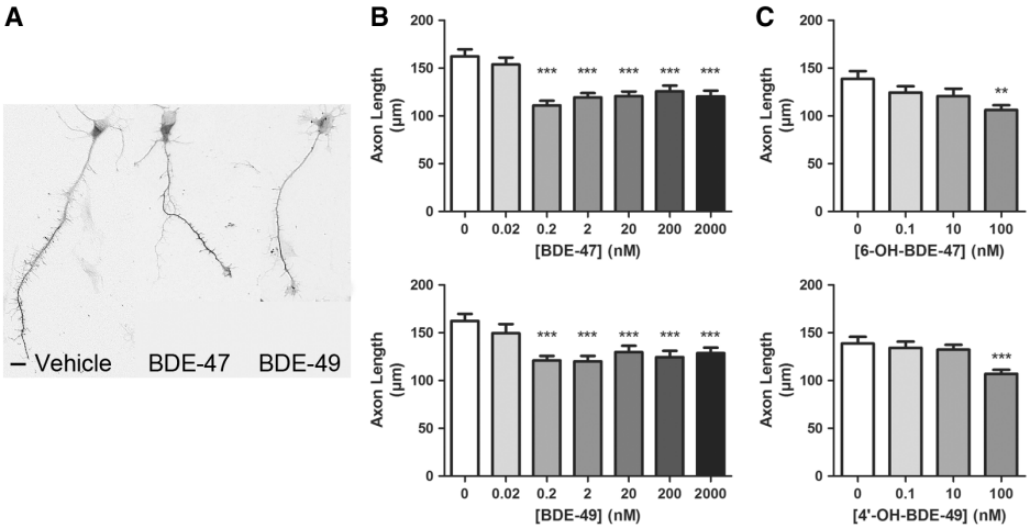

FIG. 2. BDE-47 and BDE-49 and their hydroxylated metabolites reduce axon length in cultured hippocampal neurons. Cells dissociated from P1 rat hippocampi were exposed to vehicle or varying concentrations of BDE-47, BDE-49, 6-OH-BDE-47, or 4′-OH-BDE-49 beginning 3 h after plating. After a 48 h exposure, DIV 2 neurons were fixed and immunostained for tau-1. **A,** Representative photomicrographs of DIV 2 hippocampal neurons exposed to vehicle, BDE-47 (200 nM) or BDE-49 (200 nM). **B,** Quantification of axon length in tau-1 immunopositive cells in cultures exposed to BDE-47 or BDE-49 or **(C)** 6-OH-BDE-47 or 4′-OH-BDE-47. Data presented as the mean ± SE (n = 70–90 neurons from 3 independent dissections in all groups except for the 20 pM group in which n = 40 neurons from 3 independent dissections). **P < .01, ***P < .001 relative to vehicle control. Scale bar = 10 μm.

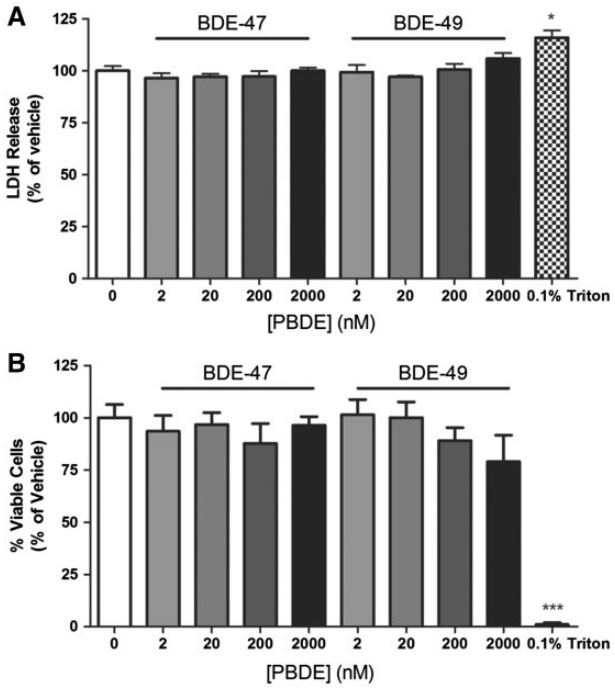

FIG. 3. BDE-47 and BDE-49 are not cytotoxic at concentrations that decrease axon length. **A,** LDH release into the media and **B,** live-dead staining using calcein AM and propidium iodide were used to assess cell viability in dissociated hippocampal cultures on DIV 2 following a 48 h exposure to vehicle or varying concentrations of BDE 47 or BDE 49. 0.1% Triton X-100 was used as a positive control. Data presented as mean ± SE (n = 3 independent dissections). *P < .05, ***P < .0001 relative to vehicle control.

parameters of cell health: LDH release (Lobner, 2000) and cellular uptake of calcein AM and propidium iodide (Vaughan *et al.*, 1995). Under the same culture conditions and PBDE exposure paradigms used for axonal growth studies, neither BDE-47 nor BDE-49 significantly altered LDH release (Figure 3A) or calcein AM and propidium iodide uptake (Figure 3B) relative to vehicle controls.

It is possible that the differential effects of BDE-47 and BDE-49 on axonal *vs.* dendritic growth reflect differential susceptibility of immature (DIV 2) versus more mature (DIV 7–9) cell cultures, respectively. To address this possibility, we tested the effects of these PBDE congeners on axonal growth following the same exposure paradigm used in the dendritic growth assays. Because it is technically challenging to quantify axonal lengths of individual neurons in mature cultures using morphometric analyses, we used western blotting to quantify expression levels of the axon-selective cytoskeletal protein tau-1 in hippocampal cultures exposed to BDE-47 or BDE-49 from DIV 7 to 9. Levels of tau-1 protein in BDE-exposed cultures were not significantly different from those in vehicle control cultures (Figure 4).

The observation that PBDEs did not significantly alter tau-1 expression in mature neurons but did decrease axonal length in immature neurons (Figure 2) suggests that these compounds interfere with very early events of axonal morphogenesis in hippocampal neurons. Previous studies have shown that hippocampal neurons in culture undergo a well-defined sequence of morphological changes to transition from an unpolarized cell with multiple "minor" neurites that are neither axonal nor dendritic into the characteristic polarized neuron with a single axonal process and multiple dendrites (Dotti *et al.*, 1988). Polarization of these neurons typically occurs over the first 24–48 h in culture, and is marked by the differentiation of one of the multiple "minor" neurites into a definable axon (Wiggin *et al.*, 2005). To assess whether PBDE effects on axon length were mediated by changes in the rate of neuronal cell polarization, hippocampal cell cultures were immunostained for GAP-43, a biomarker of axonal growth cones (Goslin and Banker, 1990; Goslin *et al.*, 1990). To score the different stages of neuronal cell polarization, we used previously described criteria based on neuronal cell morphology and the subcellular distribution of GAP-43 immunoreactivity (Goslin and Banker, 1990; Goslin *et al.*, 1990; Harrill *et al.*, 2013). Briefly, polarization was scored as

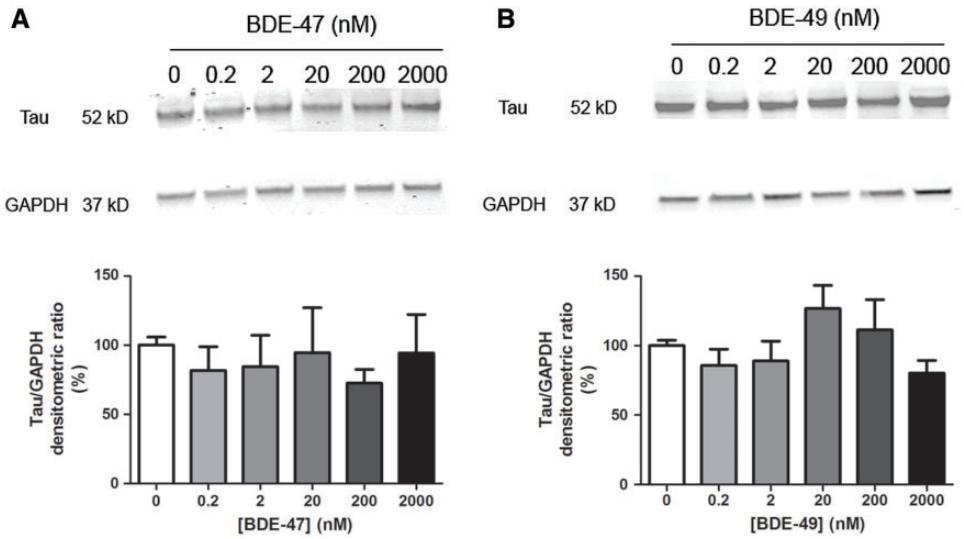

FIG. 4. BDE-47 and BDE-49 do not decrease tau-1 protein in mature cultures. At DIV 7, hippocampal neurons were exposed to BDE-47 **(A)** or BDE-49 **(B)** for 48 h. At the end of the exposure, cells were lysed for western blotting and probed with antibodies specific for tau-1 (axonal cytoskeletal protein) and GAPDH (loading control) as shown in representative western blots (top panels). Bar graphs (bottom panel) represent densitometric data. Densitometric values of tau-1 immunopositive bands were normalized to densitometric values for GAPDH immunopositive bands within the same sample. Data presented as mean ± SE (n = 3 independent dissections). ***$P < .001$ relative to vehicle control.

Stage 1 if GAP-34 immunoreactivity was localized to the cell body with no discernable immunostaining of neurites; Stage 2, if GAP-43 immunoreactivity was obvious in all neurites and no one neurite was significantly longer than the others; or Stage 3, if GAP-43 immunoreactivity was most robust in the growth cone of a single neurite that was significantly longer than the remaining neurites (Figure 5A). Stage 3 marks the initial polarization of the neuron when the GAP-43 immunopositive neurite becomes the axon (Dotti *et al.*, 1988; Goslin and Banker, 1990). Under the culture conditions used for our studies of PBDE effects on axonal growth, the majority of neurons (>75%) reached Stage 3, or became polarized, within 48 h after plating (Figure 5B). Therefore, in experiments examining the effects of PBDE exposure on neuronal cell polarization, we examined cultures at DIV 2. In cultures exposed to either BDE-47 or BDE-49 at 200 nM for 48 h beginning 3 h after plating, there were significantly fewer neurons that had reached stage 3 (or became polarized) by DIV 2 relative to vehicle control cultures (Figure 5C).

PBDE Effects on Axonal Growth Are Mediated by RyR-Dependent Mechanisms

Cytosolic Ca^{2+} plays an important role in axonal growth and guidance (Hong et al., 2000; Zheng and Poo, 2007). Since it has previously been shown that PBDEs disrupt Ca^{2+} homeostasis (Coburn et al., 2008; Dingemans *et al.*, 2010b; Dingemans *et al.*, 2011; Kim *et al.*, 2011), we hypothesized that PBDE effects on axonal growth are mediated by changes in intracellular Ca^{2+} levels ($[Ca^{2+}]_i$). To test this hypothesis, we used pharmacological antagonists of various Ca^{2+} ion channels previously implicated in PBDE developmental neurotoxicity (Hendriks and Westerink, 2015) to determine their possible involvement in the axon inhibitory effects of BDE-47 and BDE-49. Hippocampal cultures were pre-incubated 30 min prior to PBDE treatment with the L-type voltage Ca^{2+} channel blocker verapamil (30 μM), the IP_3 receptor blocker xestospongin C (1 μM) or the RyR blocker FLA365 (10 μM). These concentrations of verapamil (Keith *et al.*, 1994; Kodavanti *et al.*, 1994), xestospongin C (Gafni *et al.*, 1997; Inglefield *et al.*, 2001) and FLA365 (Chiesi *et al.*, 1988; Mack *et al.*, 1992) have previously been shown to block neuronal Ca^{2+} signaling. In the absence of PBDEs, none of these pharmacological blockers altered basal levels of axonal growth relative to vehicle controls (Figure 6A). Pretreatment of PBDE-exposed cultures with either verapamil or xestospongin did not prevent the inhibitory effects of BDE-47 and BDE-49 on axonal growth; in contrast, pretreatment with FLA365 blocked the inhibitory effects of both PBDE congeners on axonal growth (Figure 6B).

FLA365 selectively blocks RyR Ca^{2+} channels, but has been reported to also interfere with L-type Ca^{2+} channels in arterial smooth muscle cells (Ostrovskaya *et al.*, 2007). Therefore, to confirm that FLA365 antagonizes the axon inhibiting activity of PBDEs via RyR Ca^{2+} channel blockade, we determined whether siRNA knockdown of RyR phenocopies FLA365 treatment. Although all 3 RyR isoforms are expressed in the brain, we have previously shown that RyR1 and RyR2 are predominantly expressed in primary neuron-glia co-cultures derived from P0 to P1 rat hippocampi (Wayman *et al.*, 2012b). To determine whether these 2 RyR isoforms are expressed in axonal growth cones, DIV 2 hippocampal cultures were immunostained using antibodies selective for RyR1 or RyR2 and co-labeled with phalloidin to identify axonal growth cones. Puncta immunoreactive for both RyR1 and RyR2 were obvious throughout the cytoplasm of the axonal growth cone and even out along the tips of the phalloidin-labeled filopodia (Figure 7A). Expression of RyR1, RyR2, or scrambled (control) siRNA did not alter axon length in vehicle control cultures. In cultures exposed to PBDEs, expression of the control siRNA did not block the axon inhibitory effect of BDE-47 or BDE-49. In contrast, expression of RyR2 siRNA blocked inhibitory effects of both BDE-47 and BDE-49 on axon length at 200 nM (Figure 7B). Expression of RyR1 siRNA appeared to partially block the inhibitory effect of these PBDEs on axon growth as evidenced by the fact that axon lengths of PBDE-exposed neurons expressing RyR1 siRNA were not significantly different from either vehicle control neurons expressing RyR1 siRNA or PBDE-exposed neurons expressing control siRNA.

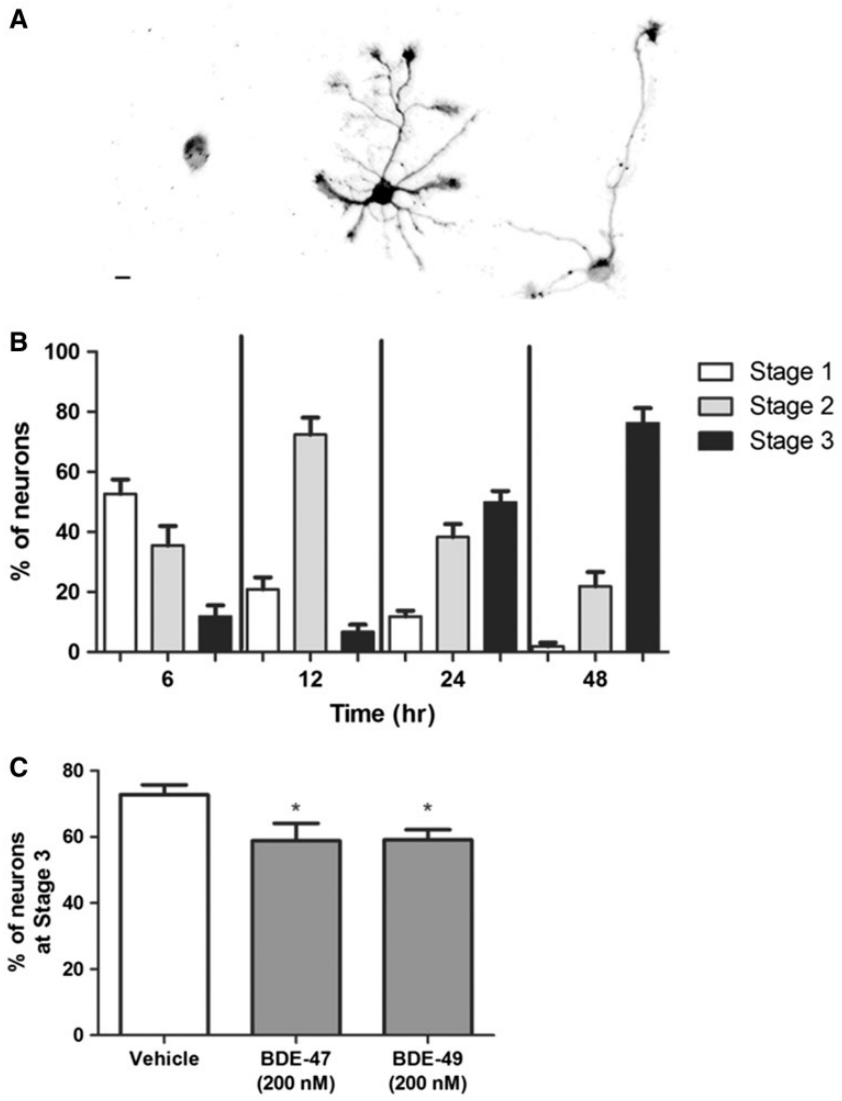

FIG. 5. BDE-47 and BDE-49 delay the development of polarity in hippocampal neurons. Polarity was quantified in dissociated hippocampal cell cultures based on the subcellular distribution of GAP-43 immunoreactivity and morphometric criteria. **A,** Representative photomicrographs of hippocampal neurons at different stages of polarization. **B,** Ontogeny of polarity in hippocampal cultures grown under the culture conditions used in this study. **C,** Percent of polarized (Stage 3) neurons at DIV 2 following a 48 h exposure to vehicle, BDE-47 (200 nM) or BDE-49 (200 nM). Data presented as mean ± SE (n = 9 coverslips collected from 3 independent dissections, 70–150 neurons each coverslip). *$P < .05$ relative to vehicle control. Scale bar = 10 μm.

DISCUSSION

Our findings support the hypothesis that PBDEs interfere with developmental processes that are critical determinants of neuronal connectivity in the developing brain. Specifically, our data demonstrate that BDE-47, BDE-49 and the hydroxylated metabolites 6-OH-BDE-47 and 4′-OH-BDE-49, inhibit the early stages of axonal growth in primary hippocampal neurons. These data extend previous reports demonstrating that the commercial PBDE mixture, DE-71, decreases neurite length in primary mouse cortical cultures (Bradner *et al.*, 2013), and that BDE-47 inhibits neurite outgrowth in human embryonic stem cell-derived neurons (Behl *et al.*, 2015) and decreases axonal length of motor neurons in larval zebrafish (Chen *et al.*, 2012). In our model, exposure to BDE-47 or BDE-49 significantly inhibits axonal growth at concentrations that have no effect on cell viability, indicating that decreased axonal growth is not due to compromised cell viability. Neither BDE-47 nor BDE-49 alters dendritic arborization, suggesting that PBDEs do not inhibit general mechanisms of neurite outgrowth, but rather they selectively target axon-specific mechanisms of growth. This observation extends previous reports demonstrating that the organophosphorus pesticide chlorpyrifos (Howard *et al.*, 2005) and the NDL PCB 136 (Yang *et al.*, 2014) differentially modulate axonal versus dendritic growth.

The axon inhibitory effect was not observed in cultures exposed to the parent PBDEs at concentrations below 200 pM or the hydroxylated metabolites at concentrations below 100 nM. Of note, the effect of PBDEs on axonal growth did not exhibit the classic sigmoidal concentration–effect relationship. Of the few published studies that have tested specific axonal effects of chemicals over a range of concentrations (Harrill *et al.*, 2013; Howard *et al.*, 2005; Pizzurro *et al.*, 2014; Yang *et al.*, 2008), all have shown a similar “all or none” or a very steep concentration–effect curve (going from no response to maximal response

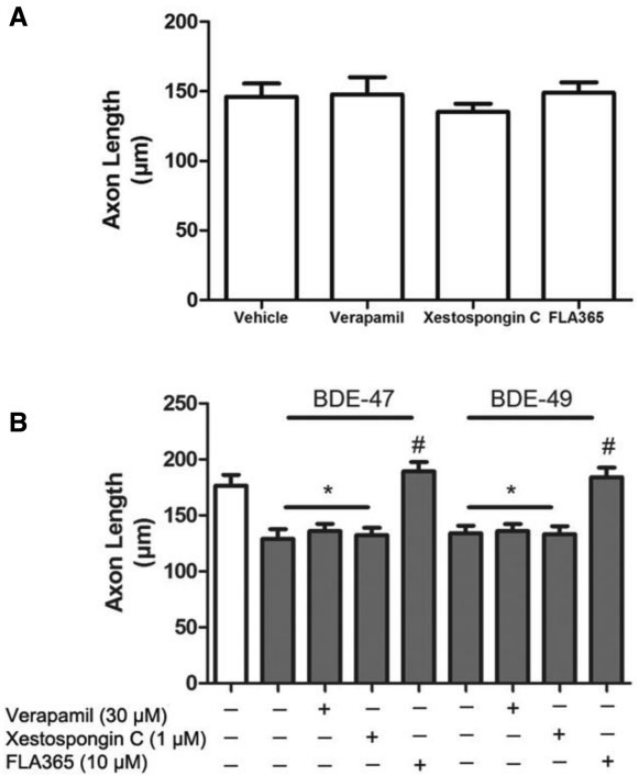

FIG. 6. Pharmacological antagonism of RyR Ca^{2+} channels blocks the inhibitory effects of BDE-47 or BDE-49 on axon length. Dissociated hippocampal cell cultures were pre-treated with the L-type Ca^{2+} channel blocker verapamil (30 μM), the IP_3 receptor blocker xestospongin C (1 μM) or the RyR blocker FLA365 (10 μM) 30 min prior to addition of vehicle, BDE-47 (200 nM) or BDE-49 (200 nM). After 48 h, cultures were fixed and immunostained for Tau-1. Axon length was quantified in cultures treated with pharmacological inhibitors in the absence **(A)** or presence **(B)** of PBDEs. Data presented as the mean ± SE (n = 30–60 neurons per condition from 3 cultures derived from a single dissection). This experiment was repeated in culture derived from 3 independent dissections with comparable results. *$P < .05$ relative to vehicle control, #$P < .05$ relative to BDE-matched cultures not treated with a pharmacological inhibitor.

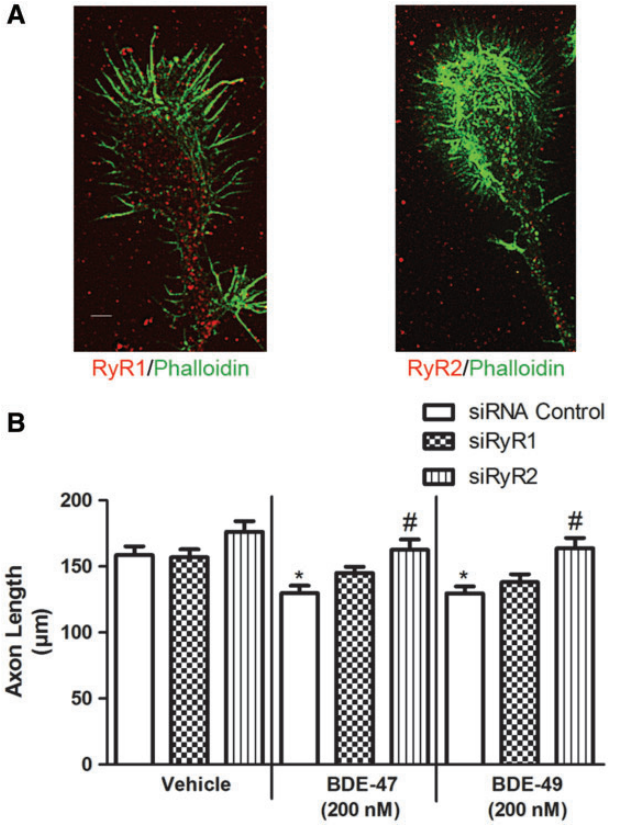

FIG. 7. BDE-47 (200 nM) and BDE-49 (200 nM) reduce axon length via RyR2-dependent mechanism(s). **A,** Representative photomicrographs of axonal growth cones in DIV 2 hippocampal cultures co-labeled with fluorescently tagged phalloidin (green) and antibody selective for RyR1 (red, left) or RyR2 (red, right). **B,** Quantitative analyses of axonal length in Cy5 positive neurons. Dissociated hippocampal cells were electroporated with Cy5-labeled scrambled (control), RYR1 or RYR2 siRNA prior to plating. Data presented as the mean ± SE (n = 90 neurons collected from 3 independent dissections). *$P < .05$ relative to vehicle control, #$P < .05$ relative to cultures transfected with control siRNA and exposed to the same BDE. Scale bar = 5 μm.

over a half-log concentration gradient). It is possible that PBDE effects on axonal growth have a steep concentration-effect relationship but we missed it because: (1) the neurons in our cultures were not synchronized with respect to their stage of polarization and/or axonal lengths at the time of exposure to PBDEs; and/or (2) our cultures are comprised of a heterogeneous population of neuronal cell types with diverse sensitivities to the axon inhibitory effects of PBDEs. However, we cannot rule out a biological basis for the concentration–effect relationship observed for the axon inhibitory effects of PBDEs.

The inhibition of axonal growth observed in primary hippocampal neurons exposed to BDE-47 or BDE-49 during the first 48 h in culture was not detected in cultures exposure from DIV 7 to 9, as quantified by western blot analyses of tau 1. Possible explanations for this difference include: (1) western blotting is not sensitive enough to detect subtle but significant differences in axonal growth; (2) mature neurons are more resistant to the growth inhibitory effects of PBDEs; (3) different cell densities were used for experiments conducted at early time points (1–2 DIV) versus later time points (7–9 DIV); and/or (4) PBDEs interfere with early but not late stages of axonal morphogenesis. Our data provide direct support for the fourth possibility: we observed that BDE-47 and BDE-49 delayed the polarization of hippocampal neurons, as evidenced by significantly lower percentages of neurons exhibiting a differentiated axon at 48 h, as determined by the redistribution of GAP-43 into a single neurite that was noticeably longer than the other "minor" neurites (Dotti *et al.*, 1988; Goslin *et al.*, 1990; Yamamoto *et al.*, 2012). This is in line with previous studies demonstrating that MARCKS, an actin-binding protein enriched in axons that co-distributes with GAP-43, is markedly decreased in rats exposed perinatally to BDE-71 (Kodavanti *et al.*, 2015; Ouimet *et al.*, 1990). These observations support a model in which PBDEs inhibit axonal growth, at least in part, by delaying neuronal polarization.

Neuronal polarization is controlled by $[Ca^{2+}]_i$, and Ca^{2+} ionophores completely suppress axon formation in primary hippocampal neurons (Mattson *et al.*, 1990). Axonal growth also requires an optimal $[Ca^{2+}]_i$ in the axonal growth cone, and $[Ca^{2+}]_i$ levels on either side of this optimum inhibit axonal growth (Kater and Mills, 1991). PBDEs are reported to alter $[Ca^{2+}]_i$ in neurons via mechanisms involving voltage-gated calcium channels, IP_3Rs and RyRs (Costa *et al.*, 2016; Dingemans *et al.*, 2010a,b; Gassmann *et al.*, 2014; Kim *et al.*, 2011). Pharmacological block of RyRs, but not L-type calcium channels or IP_3Rs, and siRNA knockdown of RyR2 prevents BDE-47 and BDE-49 inhibition of axonal growth, suggesting that these PBDEs inhibit axonal growth by sensitizing RyRs. Interestingly, RyR2 siRNA completely blocks, while RyR1 siRNA only partially

blocks, the axon inhibitory effects of BDE 47 and BDE 49. Although immunohistochemical localization data indicate that both RyR isoforms are expressed in axonal growth cones, the siRNA knockdown data suggest that RyR regulation of neuronal polarity and/or axonal growth is isoform specific. In light of a recent report that early axonal development in primary rat hippocampal neurons requires RyR-mediated transient changes in Ca^{2+} microdomains localized to the axonal growth cone (Wilson *et al.*, 2016), our data suggest a model in which RyR sensitization by BDE-47 or BDE-49 alters local Ca^{2+} dynamics in the axonal growth cone during early stages of axon development to move $[Ca^{2+}]_i$ away from the optimal levels needed for axonal specification and/or initial growth. Consistent with this model, which predicts that PBDEs modulate transient and spatially restricted changes in Ca^{2+} microdomains, using high content imaging, we were not able to detect significantly increased $[Ca^{2+}]_i$ in either the soma or axonal growth cones of primary hippocampal neurons exposed to BDE-47 or BDE-49 at concentrations that inhibit axonal growth (Supplementary Figure S4).

This study yielded several unexpected findings. First, the concentration–effect relationships of BDE-47 and BDE-49 on axonal growth are comparable despite reported differences in their potency at the RyR (Kim *et al.*, 2011). However, the initial studies that reported different RyR potencies for BDE-47 versus BDE-49 relied on receptor binding assays (Kim *et al.*, 2011). Recent work evaluating RyR-active PCBs using single channel voltage clamp to assess direct influences on channel gating kinetics (Holland *et al.*, 2016) suggests that structure activity relationships based on receptor binding assays underestimate RyR potency and are not necessarily predictive of relative potencies of RyR-active PCBs in terms of channel gating activity. Although a similar analysis has yet to be applied to PBDEs, it does raise the possibility that BDE-47 may be more potent towards the RyR than previously reported. Another possibility is that BDE-47 is metabolized in our culture model to hydroxylated forms shown to sensitize RyRs (Kim *et al.*, 2011) and to be more potent than the parent compound in increasing neuronal $[Ca^{2+}]_i$ (Dingemans *et al.*, 2008; Gassmann *et al.*, 2014). However, this seems unlikely since 6-OH-BDE-47 and 4′-OH-BDE-49 were significantly less potent than the corresponding parent compounds in reducing axon lengths. Moreover, preliminary GC/MS analysis of neuron-glia co-cultures exposed to BDE-47 or BDE-49 for 48 h did not detect hydroxylated metabolites of BDE-47 and BDE-49 (data not shown).

An alternative possibility is that the RyR is not the primary molecular target but rather a downstream effector. PBDEs have several Ca^{2+}-independent effects, including thyroid hormone dysfunction, oxidative stress and altered neurotransmission (Costa *et al.*, 2014; Hendriks and Westerink, 2015), which have been reported in non-neuronal models to modulate RyR activity (Pessah *et al.*, 2010). This possibility is supported by reports that RyR-dependent axonal development in primary hippocampal neurons is regulated upstream by physiological levels of ROS generated by NADPH oxidase-2 (Wilson *et al.*, 2016). This may also explain the second surprising observation, which is that PBDEs and NDL-PCBs have different effects on neuronal morphogenesis. As we previously demonstrated in primary hippocampal neurons, NDL PCBs enhance dendritic growth via RyR-dependent mechanisms but have no effect on axonal growth (Wayman *et al.*, 2012b; Yang *et al.*, 2014). In contrast, using the same model system, we show here that BDE-47 and BDE-49 inhibit axonal growth via RyR-dependent mechanisms but have no effect on dendritic arborization. If RyRs are an intermediary signaling molecule rather than the primary molecular target for PBDEs, it would not be surprising that PBDEs do not phenocopy NDL PCB effects on neuronal morphogenesis. Alternatively, RyR activity is regulated by numerous accessory proteins (Pessah *et al.*, 2010), and NDL PCB interactions with the RyR require the presence of the FKBP12 accessory protein (Samso *et al.*, 2009; Wong *et al.*, 1997b). Although our earlier study suggests that PBDE interactions with the RyR similarly require FKBP12 (Kim *et al.*, 2011), possibly additional accessory proteins are involved, and the profile of accessory proteins required for RyR interactions differs between NDL PCBs and PBDEs. Since the complement of RyR accessory proteins varies depending on the RyR isoform, and the subcellular compartment (Berridge, 2006; Pessah *et al.*, 2010), this explanation would be consistent with our observation that both RyR1 and RyR2 activity are required for the dendrite promoting activity of NDL PCBs (Wayman *et al.*, 2012b), while only RyR2 is required for the axon inhibiting effects of PBDEs. A related possibility derives from observations that the kinetics of changes in $[Ca^{2+}]_i$ influence the profile of activated downstream effectors (Berridge, 2006; Mattson, 1992). If the kinetics of PBDE effects on RyR gating are different than those of NDL PCBs, they could activate unique downstream effectors, resulting in differential effects on axons *vs.* dendrites. Future mechanistic studies are warranted to distinguish the relative contributions of these possibilities to the distinct toxicological profiles of PBDEs versus NDL PCBs.

The human relevance of these *in vitro* mechanistic studies is suggested by the observation that both BDE-47 and BDE-49 were observed to inhibit axonal growth at concentrations as low as 0.2 nM, which are well within the range of PBDE plasma concentrations detected in highly exposed human populations (Eskenazi *et al.*, 2011, 2013; Hertz-Picciotto *et al.*, 2011). Whether PBDE effects on axon growth contribute to neurobehavioral deficits associated with developmental exposure remains to be determined. However, evidence that spatiotemporal patterns in axonal growth can cause persistent changes in brain patterning and connectivity (Berger-Sweeney and Hohmann, 1997; Cremer *et al.*, 1997; Maier *et al.*, 1999), and are linked to neurodevelopmental disorders (Copf, 2016; Robichaux and Cowan, 2014), supports the possibility that inhibition of axonal growth is important in PBDE developmental neurotoxicity.

SUPPLEMENTARY DATA

Supplementary data are available at *Toxicological Sciences* online.

ACKNOWLEDGMENTS

The authors thank Dr Kimberly P. Keil (UC Davis) and Dr Keri A. Hayakawa (UC Davis) for providing helpful feedback on early drafts of the manuscript and Dr Yanping Lin (UC Davis) for providing preliminary GC/MS analysis of hydroxylated PBDEs.

FUNDING

This work was supported by the National Institute of Environmental Health Sciences [grant numbers R01 ES014901, P01 ES011269, P42 ES04699, U54 HD079125, F32 ES024676 to K.M.S., T32-MH073124 (postdoctoral fellowship) to K.M.S., and T32 ES007059 (predoctoral fellowship) to H.C.], the United States Environmental Protection Agency [grant numbers RD835550 and RD83543201] and the J.B. Johnson Foundation [unrestricted gift to P.J.L.]. The sponsors were not involved in the study design, the collection, analysis, and interpretation of data, in the

writing of the report or in the decision to submit the article for publication.

REFERENCES

Adasme, T., Haeger, P., Paula-Lima, A. C., Espinoza, I., Casas-Alarcon, M. M., Carrasco, M. A., and Hidalgo, C. (2011). Involvement of ryanodine receptors in neurotrophin-induced hippocampal synaptic plasticity and spatial memory formation. *Proc. Natl. Acad. Sci. U. S. A.* **108**, 3029–3034.

Behl, M., Hsieh, J. H., Shafer, T. J., Mundy, W. R., Rice, J. R., Boyd, W. A., Freedman, J. H., Hunter, E. S., 3rd, Jarema, K. A., Padilla, S., *et al.* (2015). Use of alternative assays to identify and prioritize organophosphorus flame retardants for potential developmental and neurotoxicity. *Neurotoxicol. Teratol.* **52**, 181–193.

Berger-Sweeney, J., and Hohmann, C. F. (1997). Behavioral consequences of abnormal cortical development: Insights into developmental disabilities. *Behav. Brain Res.* **86**, 121–142.

Berghuis, S. A., Bos, A. F., Sauer, P. J., and Roze, E. (2015). Developmental neurotoxicity of persistent organic pollutants: An update on childhood outcome. *Arch. Toxicol.* **89**, 687–709.

Berridge, M. J. (2006). Calcium microdomains: Organization and function. *Cell Calcium* **40**, 405–412.

Bradner, J. M., Suragh, T. A., and Caudle, W. M. (2013). Alterations to the circuitry of the frontal cortex following exposure to the polybrominated diphenyl ether mixture, DE-71. *Toxicology* **312**, 48–55.

Chandrasekaran, V., Lea, C., Sosa, J. C., Higgins, D., and Lein, P. J. (2015). Reactive oxygen species are involved in BMP-induced dendritic growth in cultured rat sympathetic neurons. *Mol. Cell Neurosci.* **67**, 116–125.

Chen, X., Huang, C., Wang, X., Chen, J., Bai, C., Chen, Y., Chen, X., Dong, Q., and Yang, D. (2012). BDE-47 disrupts axonal growth and motor behavior in developing zebrafish. *Aquat. Toxicol.* **120-121**, 35–44.

Chiesi, M., Schwaller, R., and Calviello, G. (1988). Inhibition of rapid Ca-release from isolated skeletal and cardiac sarcoplasmic reticulum (SR) membranes. *Biochem. Biophys. Res. Commun.* **154**, 1–8.

Coburn, C. G., Curras-Collazo, M. C., and Kodavanti, P. R. (2008). In vitro effects of environmentally relevant polybrominated diphenyl ether (PBDE) congeners on calcium buffering mechanisms in rat brain. *Neurochem. Res.* **33**, 355–364.

Copf, T. (2016). Impairments in dendrite morphogenesis as etiology for neurodevelopmental disorders and implications for therapeutic treatments. *Neurosci. Biobehav. Rev.* **68**, 946–978.

Costa, L. G., de Laat, R., Tagliaferri, S., and Pellacani, C. (2014). A mechanistic view of polybrominated diphenyl ether (PBDE) developmental neurotoxicity. *Toxicol. Lett.* **230**, 282–294.

Costa, L. G., Tagliaferri, S., Roque, P. J., and Pellacani, C. (2016). Role of glutamate receptors in tetrabrominated diphenyl ether (BDE-47) neurotoxicity in mouse cerebellar granule neurons. *Toxicol. Lett.* **241**, 159–166.

Cremer, H., Chazal, G., Goridis, C., and Represa, A. (1997). NCAM is essential for axonal growth and fasciculation in the hippocampus. *Mol. Cell Neurosci.* **8**, 323–335.

Dingemans, M. M., de Groot, A., van Kleef, R. G., Bergman, A., van den Berg, M., Vijverberg, H. P., and Westerink, R. H. (2008). Hydroxylation increases the neurotoxic potential of BDE-47 to affect exocytosis and calcium homeostasis in PC12 cells. *Environ. Health Perspect.* **116**, 637–643.

Dingemans, M. M., Heusinkveld, H. J., Bergman, A., van den Berg, M., and Westerink, R. H. (2010a). Bromination pattern of hydroxylated metabolites of BDE-47 affects their potency to release calcium from intracellular stores in PC12 cells. *Environ. Health Perspect.* **118**, 519–525.

Dingemans, M. M., van den Berg, M., Bergman, A., and Westerink, R. H. (2010b). Calcium-related processes involved in the inhibition of depolarization-evoked calcium increase by hydroxylated PBDEs in PC12 cells. *Toxicol. Sci.* **114**, 302–309.

Dingemans, M. M., van den Berg, M., and Westerink, R. H. (2011). Neurotoxicity of brominated flame retardants: (In)direct effects of parent and hydroxylated polybrominated diphenyl ethers on the (developing) nervous system. *Environ. Health Perspect.* **119**, 900–907.

Dotti, C. G., Sullivan, C. A., and Banker, G. A. (1988). The establishment of polarity by hippocampal neurons in culture. *J. Neurosci.* **8**, 1454–1468.

EFSA. (2011). Scientific opinion on polybrominated diphenyl ethers (PBDEs) in food. *efsa J.* **9**, 274.

Eskenazi, B., Chevrier, J., Rauch, S. A., Kogut, K., Harley, K. G., Johnson, C., Trujillo, C., Sjodin, A., and Bradman, A. (2013). In utero and childhood polybrominated diphenyl ether (PBDE) exposures and neurodevelopment in the CHAMACOS study. *Environ. Health Perspect.* **121**, 257–262.

Eskenazi, B., Fenster, L., Castorina, R., Marks, A. R., Sjodin, A., Rosas, L. G., Holland, N., Guerra, A. G., Lopez-Carillo, L., and Bradman, A. (2011). A comparison of PBDE serum concentrations in Mexican and Mexican-American children living in California. *Environ. Health Perspect.* **119**, 1442–1448.

Florvall, L., Ask, A. L., Ogren, S. O., and Ross, S. B. (1977). Selective monoamine oxidase inhibitors. *J. Med. Chem.* **21**, 56–63.

Gafni, J., Munsch, J. A., Lam, T. H., Catlin, M. C., Costa, L. G., Molinski, T. F., and Pessah, I. N. (1997). Xestospongins: Potent membrane permeable blockers of the inositol 1,4,5-trisphosphate receptor. *Neuron* **19**, 723–733.

Gassmann, K., Schreiber, T., Dingemans, M. M., Krause, G., Roderigo, C., Giersiefer, S., Schuwald, J., Moors, M., Unfried, K., Bergman, A., *et al.* (2014). BDE-47 and 6-OH-BDE-47 modulate calcium homeostasis in primary fetal human neural progenitor cells via ryanodine receptor-independent mechanisms. *Arch. Toxicol.* **88**, 1537–1548.

Goldberg, J. L. (2003). How does an axon grow?. *Genes Dev.* **17**, 941–958.

Goslin, K., and Banker, G. (1990). Rapid changes in the distribution of GAP-43 correlate with the expression of neuronal polarity during normal development and under experimental conditions. *J. Cell Biol.* **110**, 1319–1331.

Goslin, K., Schreyer, D. J., Skene, J. H., and Banker, G. (1990). Changes in the distribution of GAP-43 during the development of neuronal polarity. *J. Neurosci.* **10**, 588–602.

Harrill, J. A., Robinette, B. L., Freudenrich, T., and Mundy, W. R. (2013). Use of high content image analyses to detect chemical-mediated effects on neurite sub-populations in primary rat cortical neurons. *Neurotoxicology* **34**, 61–73.

Hayashi, K., Kawai-Hirai, R., Ishikawa, K., and Takata, K. (2002). Reversal of neuronal polarity characterized by conversion of dendrites into axons in neonatal rat cortical neurons in vitro. *Neuroscience* **110**, 7–17.

Hendriks, H. S., and Westerink, R. H. (2015). Neurotoxicity and risk assessment of brominated and alternative flame retardants. *Neurotoxicol. Teratol.* **52**, 248–269.

Hertle, D. N., and Yeckel, M. F. (2007). Distribution of inositol-1,4,5-trisphosphate receptor isotypes and ryanodine receptor isotypes during maturation of the rat hippocampus. *Neuroscience* **150**, 625–638.

Hertz-Picciotto, I., Bergman, A., Fangstrom, B., Rose, M., Krakowiak, P., Pessah, I., Hansen, R., and Bennett, D. H. (2011). Polybrominated diphenyl ethers in relation to autism and developmental delay: A case-control study. *Environ. Health* **10**, 1.

Holland, E. B., Feng, W., Zheng, J., Dong, Y., Li, X., Lehmler, H. J., and Pessah, I. N. (2016). An extended structure-activity relationship of non-dioxin-like PCBs evaluates and supports modeling predictions and identifies picomolar potency of PCB 202 towards ryanodine receptors. *Toxicol. Sci.* **155**(1):170-181.

Hong, K., Nishiyama, M., Henley, J., Tessier-Lavigne, M., and Poo, M. (2000). Calcium signalling in the guidance of nerve growth by netrin-1. *Nature* **403**, 93–98.

Howard, A. S., Bucelli, R., Jett, D. A., Bruun, D., Yang, D., and Lein, P. J. (2005). Chlorpyrifos exerts opposing effects on axonal and dendritic growth in primary neuronal cultures. *Toxicol. Appl. Pharmacol.* **207**, 112–124.

Inglefield, J. R., Mundy, W. R., and Shafer, T. J. (2001). Inositol 1,4,5-triphosphate receptor-sensitive Ca(2+) release, store-operated Ca(2+) entry, and cAMP responsive element binding protein phosphorylation in developing cortical cells following exposure to polychlorinated biphenyls. *J. Pharmacol. Exp. Ther.* **297**, 762–773.

Kapfhammer, J. P. (2004). Cellular and molecular control of dendritic growth and development of cerebellar Purkinje cells. *Prog. Histochem. Cytochem.* **39**, 131–182.

Kater, S. B., and Mills, L. R. (1991). Regulation of growth cone behavior by calcium. *J. Neurosci.* **11**, 891–899.

Keith, R. A., Mangano, T. J., DeFeo, P. A., Ernst, G. E., and Warawa, E. J. (1994). Differential inhibition of neuronal calcium entry and [3H]-D-aspartate release by the quaternary derivatives of verapamil and emopamil. *Br. J. Pharmacol.* **113**, 379–384.

Kim, K. H., Bose, D. D., Ghogha, A., Riehl, J., Zhang, R., Barnhart, C. D., Lein, P. J., and Pessah, I. N. (2011). Para- and ortho-substitutions are key determinants of polybrominated diphenyl ether activity toward ryanodine receptors and neurotoxicity. *Environ. Health Perspect.* **119**, 519–526.

Kodavanti, P. R., and Curras-Collazo, M. C. (2010). Neuroendocrine actions of organohalogens: Thyroid hormones, arginine vasopressin, and neuroplasticity. *Front. Neuroendocrinol.* **31**, 479–496.

Kodavanti, P. R., Royland, J. E., Osorio, C., Winnik, W. M., Ortiz, P., Lei, L., Ramabhadran, R., and Alzate, O. (2015). Developmental exposure to a commercial PBDE mixture: Effects on protein networks in the cerebellum and hippocampus of rats. *Environ. Health Perspect.* **123**, 428–436.

Kodavanti, P. R., Shafer, T. J., Ward, T. R., Mundy, W. R., Freudenrich, T., Harry, G. J., and Tilson, H. A. (1994). Differential effects of polychlorinated biphenyl congeners on phosphoinositide hydrolysis and protein kinase C translocation in rat cerebellar granule cells. *Brain Res.* **662**, 75–82.

Lein, P. J., Banker, G. A., and Higgins, D. (1992). Laminin selectively enhances axonal growth and accelerates the development of polarity by hippocampal neurons in culture. *Brain Res. Dev. Brain Res.* **69**, 191–197.

Lobner, D. (2000). Comparison of the LDH and MTT assays for quantifying cell death: Validity for neuronal apoptosis?. *J. Neurosci. Methods* **96**, 147–152.

Lohmann, C., and Wong, R. O. (2005). Regulation of dendritic growth and plasticity by local and global calcium dynamics. *Cell Calcium* **37**, 403–409.

Mack, W. M., Zimanyi, I., and Pessah, I. N. (1992). Discrimination of multiple binding sites for antagonists of the calcium release channel complex of skeletal and cardiac sarcoplasmic reticulum. *J. Pharmacol. Exp. Ther.* **262**, 1028–1037.

Maier, D. L., Mani, S., Donovan, S. L., Soppet, D., Tessarollo, L., McCasland, J. S., and Meiri, K. F. (1999). Disrupted cortical map and absence of cortical barrels in growth-associated protein (GAP)-43 knockout mice. *Proc Natl Acad Sci U. S. A.* **96**, 9397–9402.

Mattson, M. P. (1992). Calcium as sculptor and destroyer of neural circuitry. *Exp. Gerontol.* **27**, 29–49.

Mattson, M. P., Murain, M., and Guthrie, P. B. (1990). Localized calcium influx orients axon formation in embryonic hippocampal pyramidal neurons. *Brain Res. Dev. Brain Res.* **52**, 201–209.

Meijering, E., Jacob, M., Sarria, J. C., Steiner, P., Hirling, H., and Unser, M. (2004). Design and validation of a tool for neurite tracing and analysis in fluorescence microscopy images. *Cytometry a* **58**, 167–176.

Miller, M. F., Chernyak, S. M., Batterman, S., and Loch-Caruso, R. (2009). Polybrominated diphenyl ethers in human gestational membranes from women in southeast Michigan. *Environ. Sci. Technol.* **43**, 3042–3046.

Mosmann, T. (1983). Rapid colorimetric assay for cellular growth and survival: Application to proliferation and cytotoxicity assays. *J. Immunol. Methods* **65**, 55–63.

Ohashi, R., Sakata, S., Naito, A., Hirashima, N., and Tanaka, M. (2014). Dendritic differentiation of cerebellar Purkinje cells is promoted by ryanodine receptors expressed by Purkinje and granule cells. *Dev. Neurobiol.* **74**, 467–480.

Ostrovskaya, O., Goyal, R., Osman, N., McAllister, C. E., Pessah, I. N., Hume, J. R., and Wilson, S. M. (2007). Inhibition of ryanodine receptors by 4-(2-aminopropyl)-3,5-dichloro-N,N-dimethylaniline (FLA 365) in canine pulmonary arterial smooth muscle cells. *J. Pharmacol. Exp. Ther.* **323**, 381–390.

Ouimet, C. C., Wang, J. K., Walaas, S. I., Albert, K. A., and Greengard, P. (1990). Localization of the MARCKS (87 kDa) protein, a major specific substrate for protein kinase C, in rat brain. *J. Neurosci.* **10**, 1683–1698.

Pessah, I. N., Cherednichenko, G., and Lein, P. J. (2010). Minding the calcium store: Ryanodine receptor activation as a convergent mechanism of PCB toxicity. *Pharmacol. Ther* **125**, 260–285.

Pizzurro, D. M., Dao, K., and Costa, L. G. (2014). Astrocytes protect against diazinon- and diazoxon-induced inhibition of neurite outgrowth by regulating neuronal glutathione. *Toxicology* **318**, 59–68.

Robichaux, M. A., and Cowan, C. W. (2014). Signaling mechanisms of axon guidance and early synaptogenesis. *Curr. Top. Behav. Neurosci.* **16**, 19–48.

Samso, M., Feng, W., Pessah, I. N., and Allen, P. D. (2009). Coordinated movement of cytoplasmic and transmembrane domains of RyR1 upon gating. *PLoS Biol.* **7**, e85.

Seymour-Laurent, K. J., and Barish, M. E. (1995). Inositol 1,4,5-trisphosphate and ryanodine receptor distributions and patterns of acetylcholine- and caffeine-induced calcium release in cultured mouse hippocampal neurons. *J. Neurosci.* **15**, 2592–2608.

Stamou, M., Streifel, K. M., Goines, P. E., and Lein, P. J. (2013). Neuronal connectivity as a convergent target of gene x environment interactions that confer risk for Autism Spectrum Disorders. *Neurotoxicol. Teratol.* **36**, 3–16.

USEPA. (2010). An Exposure Assessment of Polybrominated Diphenyl Ethers. EPA/600-R-086F, May 2010. Washington DC: National Center for Environmental Assessment, Office of Research and Development, U.S. Environmental Protection Agency.

Valnegri, P., Puram, S. V., and Bonni, A. (2015). Regulation of dendrite morphogenesis by extrinsic cues. *Trends Neurosci.* **38**, 439–447.

Vaughan, P. J., Pike, C. J., Cotman, C. W., and Cunningham, D. D. (1995). Thrombin receptor activation protects neurons and astrocytes from cell death produced by environmental insults. *J. Neurosci.* **15**, 5389–5401.

Wayman, G. A., Bose, D. D., Yang, D., Lesiak, A., Bruun, D., Impey, S., Ledoux, V., Pessah, I. N., and Lein, P. J. (2012a). PCB-95 modulates the calcium-dependent signaling pathway responsible for activity-dependent dendritic growth. *Environ. Health Perspect.* **120**, 1003–1009.

Wayman, G. A., Impey, S., Marks, D., Saneyoshi, T., Grant, W. F., Derkach, V., and Soderling, T. R. (2006). Activity-dependent dendritic arborization mediated by CaM-kinase I activation and enhanced CREB-dependent transcription of Wnt-2. *Neuron* **50**, 897–909.

Wayman, G. A., Yang, D., Bose, D. D., Lesiak, A., Ledoux, V., Bruun, D., Pessah, I. N., and Lein, P. J. (2012b). PCB-95 promotes dendritic growth via ryanodine receptor-dependent mechanisms. *Environ. Health Perspect.* **120**, 997–1002.

Wiggin, G. R., Fawcett, J. P., and Pawson, T. (2005). Polarity proteins in axon specification and synaptogenesis. *Dev. Cell* **8**, 803–816.

Wilson, C., Munoz-Palma, E., Henriquez, D. R., Palmisano, I., Nunez, M. T., Di Giovanni, S., and Gonzalez-Billault, C. (2016). A feed-forward mechanism involving the NOX complex and RyR-mediated Ca2+ release during axonal specification. *J. Neurosci.* **36**, 11107–11119.

Wong, P. W., Brackney, W. R., and Pessah, I. N. (1997a). Ortho-substituted polychlorinated biphenyls alter microsomal calcium transport by direct interaction with ryanodine receptors of mammalian brain. *J. Biol. Chem.* **272**, 15145–15153.

Wong, P. W., Joy, R. M., Albertson, T. E., Schantz, S. L., and Pessah, I. N. (1997b). Ortho-substituted 2,2',3,5',6-pentachlorobiphenyl (PCB 95) alters rat hippocampal ryanodine receptors and neuroplasticity in vitro: Evidence for altered hippocampal function. *Neurotoxicology* **18**, 443–456.

Wong, P. W., and Pessah, I. N. (1996). Ortho-substituted polychlorinated biphenyls alter calcium regulation by a ryanodine receptor-mediated mechanism: Structural specificity toward skeletal- and cardiac-type microsomal calcium release channels. *Mol. Pharmacol.* **49**, 740–751.

Yamamoto, H., Demura, T., Morita, M., Banker, G. A., Tanii, T., and Nakamura, S. (2012). Differential neurite outgrowth is required for axon specification by cultured hippocampal neurons. *J. Neurochem.* **123**, 904–910.

Yang, D., Howard, A., Bruun, D., Ajua-Alemanj, M., Pickart, C., and Lein, P. J. (2008). Chlorpyrifos and chlorpyrifos-oxon inhibit axonal growth by interfering with the morphogenic activity of acetylcholinesterase. *Toxicol. Appl. Pharmacol.* **228**, 32–41.

Yang, D., Kania-Korwel, I., Ghogha, A., Chen, H., Stamou, M., Bose, D. D., Pessah, I. N., Lehmler, H. J., and Lein, P. J. (2014). PCB 136 atropselectively alters morphometric and functional parameters of neuronal connectivity in cultured rat hippocampal neurons via ryanodine receptor-dependent mechanisms. *Toxicol. Sci.* **138**, 379–392.

Yang, D., Kim, K. H., Phimister, A., Bachstetter, A. D., Ward, T. R., Stackman, R. W., Mervis, R. F., Wisniewski, A. B., Klein, S. L., Kodavanti, P. R., *et al.* (2009). Developmental exposure to polychlorinated biphenyls interferes with experience-dependent dendritic plasticity and ryanodine receptor expression in weanling rats. *Environ. Health Perspect.* **117**, 426–435.

Zheng, J. Q., and Poo, M. M. (2007). Calcium signaling in neuronal motility. *Annu. Rev. Cell Dev. Biol.* **23**, 375–404.